Gut-associated bacteria invade the midgut epithelium of *Aedes aegypti* and stimulate innate immunity and suppress Zika virus infection in cells.

Shivanand Hegde[1,2], Denis Voronin[3], Aitor Casas-Sanchez[1,2] Miguel A. Saldaña[4], Eva Heinz[1,5], Alvaro Acosta-Serrano[1,2], Vsevolod L. Popov[6], Ashok K. Chopra[4], Grant L. Hughes[1,2#]

[1]Department of Vector Biology, Liverpool School of Tropical Medicine, Liverpool, United Kingdom

[2]Department of Tropical Disease Biology, Liverpool School of Tropical Medicine, Liverpool, United Kingdom

[3]Laboratory of Molecular Parasitology, New York Blood Center, New York, NY, USA

[4]Department of Microbiology and Immunology, University of Texas Medical Branch, Galveston, TX, USA.

[5]Department of Clinical Sciences, Liverpool School of Tropical Medicine, Liverpool, United Kingdom.

[6]Department of Pathology, University of Texas Medical Branch, Galveston, TX, USA.

[#]Corresponding author. Grant Hughes: grant.hughes@lstmed.ac.uk

Abstract

Microbiota within mosquitoes influence nutrition, immunity, fecundity, and the capacity to transmit pathogens. Despite their importance, we have a limited understanding of host-microbiota interactions, especially at the cellular level. It is evident bacterial symbionts that are localized within the midgut also infect other organs within the mosquito; however, the route these symbionts take to colonize other tissues is unknown. Here, utilizing the gentamicin protection assay, we showed that the bacterial symbionts *Cedecea* and *Serratia* have the capacity to invade and reside intracellularly within mosquito cells. Symbiotic bacteria were found within a vacuole and bacterial replication was observed in mosquito cell by transmission electron microscopy, indicating bacteria were adapted to the intracellular milieu. Using gene silencing, we determined that bacteria exploited host factors, including actin and integrin receptors, to actively invade mosquito cells. As microbiota can affect pathogens within mosquitoes, we examined the influence of intracellular symbionts on Zika virus (ZIKV) infection. Mosquito cells harbouring intracellular bacteria had significantly less ZIKV compared to uninfected cells or cells exposed to non-invasive bacteria. Intracellular bacteria were observed to substantially upregulate the Toll and IMD innate immune pathways, providing a possible mechanism mediating these anti-viral effects. Examining mono-axenically infected mosquitoes using transmission electron and fluorescent microscopy revealed that bacteria occupied an intracellular niche *in vivo*. Our results provided evidence that bacteria that associate with the midgut of mosquitoes have intracellular lifestyles which likely have implications for mosquito biology and pathogen infection. This study expands our understanding of host-microbiota interactions in mosquitoes,

which is important as symbiont microbes are being exploited for vector control strategies.

Introduction

Mosquitoes are holometabolous insects with aquatic and terrestrial life stages. Aquatic stages are continually exposed to microbes in the larval habitat while adults likely acquire microbiota from the environment after eclosion or when nectar feeding [1-3]. Additionally, environmentally acquired microbes may persist in mosquito tissues between aquatic and adult life states facilitating transstadial transmission [4-6]. It is likely that these processes contribute to the considerable variability seen in the adult microbiome [7-9]. While our understanding of genetic factors that influence host-microbe interactions and microbiome acquisition are expanding [10, 11], we still have a poor knowledge of these interactions at the cellular level. Given the importance of the microbiome on mosquito traits relevant for vectorial capacity and vector competence [12-15], understanding processes that influence microbiome homeostasis is critical for developing microbial-based control strategies [16, 17].

Bacterial microbiota often resides within several organs in mosquitoes and appears to be able to migrate between tissues. Several studies have identified bacteria in the gut of mosquitoes [9, 18-20], which have led to these microbes being commonly referred to as gut microbes, but many of these bacterial species also colonize other tissues such as the salivary gland [18, 20-23], reproductive tract [20, 22, 24], or malpighian tubules [4]. While some bacteria are unique to each tissue, several infect multiple tissues within the mosquito [20, 25], and localization in organs such as the malpighian tubules and reproductive tissues likely enables transmission between life stages and generations, respectively. Both *Asaia* and *Serratia* are transferred vertically to progeny after

72 administered to the mosquito in a sugar meal, suggesting symbiotic bacteria have the
73 capacity to translocate from the midgut to the germline of their host [20, 26-28].
74 However, mechanisms facilitating their translocation remain elusive. Infection of the
75 entomopathogic fungus *Beavaria* of *Anopheles* mosquitoes enabled *Serratia* to escape
76 the midgut and over replicate in the hemolymph, which was the cause of mortality to the
77 insect [29]. In *Drosophila*, orally infected *Serratia* localized within the midgut epithelium
78 [30]. While the epithelial infection was rare in wild type flies, *Serratia* was observed to
79 localize intracellularly in *imd* knock-out flies, suggesting that host immunity influenced
80 cellular localization or controlled infections [30]. Although intracellular bacterial
81 infections have been observed in the midgut of flies [30], cellularity of gut-associated
82 bacterial infections in mosquitoes and the mechaimism facilitating systemic infection of
83 different tissues is largely unknown. It is plausible that an intracellular lifestyle could
84 provide a mechanism for transstadial and vertical transmission of bacteria in mosquito
85 vectors.
86
87 In mammalian systems, bacteria exploit their invasive capability to colonize host tissue
88 and systemically spread within multicellular organisms [31-33]. Pathogenic bacteria like
89 *Listeria, Salmonella, Vibrio,* and *Yersinia* invade host cells to colonize, replicate, and
90 migrate between cells [32]. While the invasive capacity and mechanisms have been
91 studied extensively in mammalian cells, *in vitro* investigation in mosquitoes or other
92 arthropod vectors is lacking. In order to obtain a more complete understanding of the
93 cellularity of bacteria associated with mosquitoes, we assessed the invasive capability
94 of two common *Enterobacteriaceae* bacteria in mosquito cells using the gentamicin

invasion assay. Using this *in vitro* assay, we characterized the invasive process, examined the mechanisms by which bacteria invade cells, and assessed the effect of intracellular bacteria on host immunity and Zika virus (ZIKV) infection. Importantly, using mono-axenically infected mosquitoes, we found that these bacteria have intracellular localization in mosquitoes. This work expands our understanding of host-microbe interactions of gut-associated symbionts in medically relevant mosquito vectors at the cellular level.

Results and Discussion

Symbiotic bacteria invade mosquito cells *in vitro*

Horizontally acquired bacteria are generally considered to infect the gut lumen, they are also found in other organs of mosquitoes including the salivary glands, malpighian tubules, and germline [3, 4, 6, 25, 34]. It remains unknown how these tissues become infected, but it has been proposed these organs may act as a reservoir to facilitate transstadial transmission of microbes between mosquito life stages [4, 5]. One possibility is that gut bacteria exploit their intracellular lifestyle to transition between host tissues. Therefore, we investigated the capacity of bacteria commonly found in the gut of mosquitoes to invade mosquito host cells. We isolated two bacteria within the *Enterobacteriaceae* family, *Serratia* sp. and *Cedecea neteri,* by conventional microbiological culturing approaches, and evaluated their invasive capacity using the gentamicin invasion assay [35].

While invasion assays are routinely used for pathogenic bacteria in mammalian cells, the assay is not commonly undertaken with mosquito cells. We performed the gentamicin invasion assay in Aag2 (*Aedes aegypti*) and Sua5B (*Anopheles gambiae*) cell lines comparing the invasion of *E. coli* BL21 (DE3) with or without the *Yersinia pseudotuberculosis* (*Yp*) *invasin* (*inv*) gene to invasion of these bacteria in Vero cells (Monkey Kidney cells). In mammalian systems, heterologous expression of the *Ypinv* gene facilitates invasion of *E. coli* into cell lines [36-38]. Similar to mammalian systems, we found that *E. coli* expressing the *Ypinv* gene had significantly increased invasion in Aag2 cells compared to the non-invasive *E. coli* control (Fig. S1, Unpaired t test, $p < 0.05$), while no statistical difference was seen in the Sua5B cell line, likely due to high variability among replicates ($p > 0.05$, Unpaired t test). As expected, *E. coli* expressing the *inv* gene invaded at significantly higher rates in Vero cells compared to non-invasive *E. coli* ($p < 0.05$, Unpaired t test). While several insect cell lines are naturally phagocytic [39, 40], our data suggested bacteria were actively invading Aag2 cells, and as such, we conducted the majority of our experiments with this cell line. Next, we completed the gentamicin invasion assay with the two gut-associated bacteria from mosquitoes, *C. neteri* and *Serratia* sp., and used *E. coli* with and without the *Ypinv* gene as the positive and negative controls, respectively. The native symbionts exhibited significantly higher rates of invasion compared to the *E. coli* expressing *Ypinv* (ANOVA with Tukey's multiple comparision test, $p < 0.05$) or wildtype *E. coli* (Fig. 1A, ANOVA with Tukey's multiple comparision test, $p < 0.01$) indicating native gut-associated microbes have the capacity to invade insect cells and are more adept at this process compared to non-native *E. coli* expressing mammalian invasive factors.

To further confirm the results from the gentamicin invasion assay, fluorescent and transmission electron microscopy (TEM) were performed on cells after invasion. In order to observe the invaded bacteria in cells using fluorescent microscopy, bacteria were transformed with a plasmid that expressed the mCherry fluorescent protein [41]. Similar to our quantitative results from the invasion assay, we observed a greater number of intracellular bacteria in the *Serratia* and *Cedecea* treatments compared to the *E. coli* negative control (Fig. 1B and Fig. S2). TEM images confirmed both symbionts isolated from mosquitoes were intracellular, and that bacteria were inside a vacuole (Fig. 1B, black arrowhead). *E. coli* did not invade cells and was found exclusively extracellularly. Bacterial encapsulation within a vacuole is a typical signature of invading bacteria in mammalian systems [42] as well as obligatory intracellular bacteria of insects such as *Wolbachia* [43]. Taken together, it is evident that both symbionts isolated from the mosquitoes can invade the host cells *in vitro*.

Next, we characterized the invasion process of *Cedecea* examining how the multiplicity of infection (MOI) and incubation time influenced invasion. We noted a linear increase in the number of intracellular *Cedecea* with increasing multiplicity of infection (MOI) (Fig. 1C, ANOVA with Tukey's multiple comparision test, $p < 0.05$). We then varied the invasion time and observed bacterial invasion as early as 15 minutes post infection and invasion increased until 8 hr post infection (Fig. 1D, ANOVA with Tukey's multiple comparision test, $p < 0.05$). We also examined the invasive ability of *C. neteri* in different mosquito cells lines. The invasion of this bacterium was similar in both *Ae.*

aegypti cell lines Aag2 and RML-12 (Fig. 1E, Tukey's multiple comparision test, $p < 0.05$); however, a greater number of intracellular bacteria were seen in the Sua5B cells.

In vitro intracellular replication and egression of *Cedecea neteri*

While undertaking TEM, we captured an image of intracellular replication of *C. neteri* within mosquito cells (Fig. 2A). Given that bacteria were seen to replicate in the intracellular environment, we attempted to culture these bacteria in Aag2 cells in a similar manner to *in vitro* propagation of other intracellular bacteria such as *Wolbachia* [44]. However, our culturing attempts were unsuccessful as the cell culture media became contaminated with the innoculated *C. neteri,* despite the extracellular bacteria, which had not invaded, being killed by gentamicin treatment. We hypothesized that intracellular *Cedecea* were egressing from the cells and replicating within the cell culture media.

We therefore undertook experiments to quantify bacterial egression from the cells. After allowing *C. neteri* to invade, Aag2 cells were incubated with or without gentamicin and intracellular and extracellular bacteria were quantified over time. Within the cell, bacterial numbers remained constant in the presence of gentamicin while in the absence of antibiotic, there was an an approximate 10-fold increase at eight hours post infection (Fig. 2B, Unpaired t test, $p<0.05$). In the cell culture media, we observed a precipitous increase in bacteria in the absence of antibiotic and recovered little to no viable bacteria when antibiotics were included in the media (Fig. 2C, Unpaired t test, $p<0.05$). These data indicated that *C. neteri* was egressing from the cells, replicating in

the cell culture media in the absence of antibiotic and then re-invading mosquito cells, which accounted for the significantly higher titer of intracellular *Cedecea* in the non-antibiotic treated cells at 8 hours post infection. We found few changes in the total number of mosquito cells in gentamicin treated or untreated cells, although there was a subtle but significant reduction in cell number after 8 hours in the treatment without antibiotics (Fig. S3, Unpaired t test, $p<0.0001$). However, overall, these data indicated that bacterial invasion and egression were not overly detrimental to the host cells.

Host actin and integrin are important for *Cedecea neteri* invasion

The lack of damage to host cells indicates non-lysis mediated exit of bacteria from host cells. While this would be expected from a mutualistic or commensal gut-associated bacterium, even some pathogens such as *Mycobacteria*, *Shigella*, and *Chlamydia* use protrusions and non-lytic exocytosis to exit the host cells without lysis of host cells [45-48]. The former method involves membrane extensions containing bacteria mediated by actin polymerization and ultimately these protruded structures are engulfed by neighboring cells resulting in the transfer of content to adjoining cell [49]. We therefore hypothesized that *C. neteri* may use actin-based motility as a mechanism to invade and exit cells.

To determine the role of the actin cytoskeleton in invasion of bacteria into mosquito cells, we inhibited the polymerization of actin filaments using cytochalasin D [50]. We observed a 3-fold reduction in invasion of *Cedecea* in the presence of cytochalasin D (Fig. 3A, ANOVA with Tukey's multiple comparision test, $p< 0.001$). In contrast, there

was no change in intracellular bacteria when cells were treated with SP600125, which inhibits phagocytosis in mosquito cells [51]. These data suggested that the actin cytoskeleton is co-opted by *C. neteri* to gain access to the intracellular milieu, and that phagocytosis played a minimal role in the invasion of bacteria. Similar processes have been observed in other bacteria-host systems. For example, obligatory intracellular bacteria such as *Rickettsia*, *Chlamydia*, and *Ehrlichia* hijack the host cell cytoskeletal and surface proteins to invade, survive and spread within cells [52-54]

We then examined whether host receptors facilitate the bacterial entry into mosquito cells. In mosquitoes, integrins are involved in the engulfment of *E. coli* and malaria parasites [55], while pathogenic bacteria of humans also exploit these receptors to invade mammalian host cells [56-58]. Using RNAi, we silenced the alpha and beta subunit of the integrin receptor and challenged cells with *C. neteri*. After confirming gene silencing (Fig. S4 A and B), we found significantly fewer intracellular bacteria after knocking down the beta-integrin (Fig. 3B, ANOVA with Tukey's multiple comparision test, $p < 0.05$), but no differences in the rate of *Cedecea* invasion when the alpha-integrin gene was silenced (Fig. 3C, ANOVA with Tukey's multiple comparision test, $p > 0.05$). These results indicated that symbiotic *C. neteri* utilized actin filaments and the beta-integrin receptor to gain entry into the host cells.

Intracellular *Cedecea* reduces ZIKV replication in mosquito cells

Midgut-associated bacteria can affect pathogens transmitted by mosquitoes by direct or indirect interactions [59-61]. Therefore, we examined how intracellular *C. neteri* affected

232 viral infection. The symbiont significantly reduced ZIKV loads in cell lines compared to
233 uninfected controls at both two (Fig. 4A, Unpaired t test, $p < 0.05$) and four (Fig. 4B,
234 Unpaired t test, $p < 0.01$) days post virus infection (dpvi) (Fig 4A and 4B). Similar to
235 *Cedecea*, intracellular *Serratia* also significantly reduced ZIKV density by four logs
236 compared to the uninfected cells at four dpvi (Fig. 4C, ANOVA with Tukey's multiple
237 comparison test, $p < 0.05$). To determine how the density of bacteria influenced viral
238 infection, we infected cells at increasing bacterial MOIs before inoculating with virus. At
239 lower MOIs (1:1 and 1:2), *Cedecea* significantly reduced ZIKV compared to the *E. coli*
240 (MOI 1:1, Unpaired t test, $p <0.01$, MOI 1:2, Unpaired t test, $p <0.0001$). However, at
241 higher MOIs, we noted that both *Cedecea* and *E. coli* reduced ZIKV compared to the
242 uninfected control. The complete blockage of ZIKV at the higher MOIs suggested that
243 even non-invasive bacteria can overwhelm viral infection, likely by induction of the
244 immune effector molecules that are antagonistic to viral infection. Taken together, our
245 results suggested that members of *Enterobacteriaceae* that commonly infect
246 mosquitoes have the capacity to interfere with viral pathogens when they are
247 intracellular.
248
249 **_Cedecea_ invasion stimulates mosquito immunity**
250 There is a complex interplay between the host innate immune system and microbiota
251 which maintains microbiome homeostasis [16, 62, 63]. However, invading arboviral
252 pathogens are also susceptible to these immune pathways [64, 65] thereby providing an
253 indirect mechanism by which microbiota can interfere with pathogens. We therefore
254 examined the immune response of mosquito cells challenged with *Cedecea* or *E. coli*

255 comparing these responses to uninfected cells. We quantified the transcription factors
256 (*rRel1*, *rRel2* and *Stat*) and negative regulators (*Cactus*, *Caspar*, and *PIAS*) of the Toll,
257 IMD and Jak/Stat immune pathways as well as downstream effector molecules
258 (*gambicin*, *definsin* and *cecropin*). We found the NF-κB transcription factor *Rel2* was
259 significantly upregulated by *Cedecea* compared to both the *E. coli* (ANOVA with Tukey's
260 multiple comparison test, $p < 0.05$) and the uninfected control (ANOVA with Tukey's
261 multiple comparison test, $p < 0.01$), while a significant difference was only observed for
262 *Rel1* when the *Cedecea* treatment was compared to the uninfected control (ANOVA
263 with Tukey's multiple comparison test, $p < 0.05$; Fig 5A). The negative regulator of the
264 Toll pathway, *Cactus*, was significantly upregulated compared to both the *E. coli* (Fig.
265 5B, ANOVA with Tukey's multiple comparison test, $P < 0.05$) and uninfected control
266 (ANOVA with Tukey's multiple comparison test, $p < 0.01$), while no changes were seen
267 for *Caspar*, the negative regulator of the IMD pathway (Fig. 5B, ANOVA with Tukey's
268 multiple comparison test, $p>0.05$,). Similarly, no significant changes were observed for
269 genes in the Jak/Stat pathway. Taken together, these data suggested that the Toll and
270 IMD pathways were induced by invasion of *Cedecea* into mosquito cells. This is
271 consistent with previous observations which demonstrated interplay between native
272 microbiota and mosquito innate immune pathways [61, 66-68]. We observed dramatic
273 modulation of effector molecules with *Defensin*, *Cecropin* and *Gambicin,* all significantly
274 enhanced by *Cedecea*. Strikingly, *Cecropin* and *Defensin* expression was nearly 1000-
275 fold higher (Fig. 5C, Tukey's multiple comparison test, $p < 0.0001$) whereas *Gambicin*
276 (Fig. 5C, Tukey's multiple comparison test, $p <0.001$) was elevated 100-fold in cells
277 inoculated with *Cedecea* compared to the non-infected control. In mosquitoes, these

downstream effector molecules are co-regulated by the Toll and IMD pathways [66], which could explain their prolific enhancement given that intracellular *Cedecea* stimulated both pathways. As arboviral pathogens also interact with innate immune pathways, we examined gene expression in cells when co-infected with ZIKV and *C. neteri* focusing on the NF-κB transcription factors and negative regulators of the Toll and IMD pathways. Patterns of gene expression were similar to the ZIKV uninfected cells with the exception of *Cactus*, where no significant differences were seen across bacterial treatments (Fig. 5D and E), suggesting that ZIKV was stimulating the Toll pathway as the negative regulator was depleted when comparing to ZIKV uninfected cells.

Intracellular *Enterobacteriaceae* within the *Aedes* gut epithelium

To determine the capacity of *C. neteri* and *Serratia* sp. to invade host cells *in vivo,* we reared *Ae. aegypti* mosquitoes mono-axenically with either symbiont and analyzed tissues from larvae and adults by TEM and Confocal Laser Scanning Microscopy (CLSM). While it was evident there was an accumulation of extracellular *Serratia* in the lumen of the larval gut (Fig. 6A-B), we also identified bacteria that were associated with the microvilli. Specifically, we found examples of *Serratia* in the process of transitioning to or from the midgut epithelial cells. We appreciate our results cannot conclusively determine if *Serratia* was in the process of invading or egressing from cells, but regardless, it suggested that the bacterium had been or was soon to be intracellular. Analysis of gut tissue isolated from adult *Ae. aegypti* mosquitoes infected with *C. neteri* revealed the presence of bacteria in the cytosol of epithelial cells (Fig. 6B). Closer

inspection of these images revealed the bacterium was localized within a vacuole (Fig. 6B, yellow insert), which is a typical signature of intracellular bacteria. Here, *C. neteri* may be exiting the membrane (Fig. 6B, inserts, white arrow), suggesting these bacteria can egress from the membrane bound compartment which could facilitate their replication and spreading.–Egression and re-entry mechanisms are used by several pathogenic bacteria like *Listeria monocytogenes* and *Shigella flexneri* to escape the vacuoles to replicative niches [69]. We also confirmed the intracellular localization of *C. neteri* in adult infected guts by CLSM. The orthogonal views of the 3D-reconstructed tissues locate bacteria on the cells as well as inside cells of the posterior gut, demonstrated by the co-localization of actin staining with mCherry signal from bacteria (Fig. 6C, Fig. S5, Supplementary video 1). We also found bacteria inside the cells of the Malpighian tubules (Fig. 6C, Fig. S5, Supplementary video 2). Altogether, TEM and CLSM results clearly show bacteria residing inside the host cells *in vivo*.

Our data show that *Enterobacteriaceae* that commonly infect the gut of mosquitoes have the capacity to invade mosquito cells *in vitro* and *in vivo*. To gain access and persist in these cells, bacteria need to overcome the host immune response and the peritrophic matrix (PM). The PM, which acts as a physical barrier that separates epithelial cells from the gut lumen, is expressed constitutively in larvae and after a blood meal in adults. In a range of arthropods, genes associated with the PM are induced by bacteria [70] and in turn, the PM plays a pivotal role maintaining gut microbiome homeostasis, either by protecting bacteria from the innate immune response or restoring bacterial composition and adundance post blood meal [71]. While another

study has identified bacteria associating with the epithelium in *Anopheles* mosquitoes [72] our finding of intracellular bacteria residing within the midgut epithelium of larvae and adults indicates the PM is not completely effective at inhibiting microbiota or that bacteria invade these cells before the PM has established. Alternatively, bacteria may produce enzymes that degrade the PM in a similar fashion to malaria parasites that express chitenases [73].

In *Drosophila*, ingested *Serratia* (Db11) invaded the midgut epithlieum in flies with an impaired IMD pathway, but not wild type flies. However, this infection reduces survival [30]. Similarly, fungal infection of *Anopheles* mosquitoes enables gut bacteria to translocate to the hemolymph leading to systemic infection [29]. Similar to the observations in *Drosophila* [30], we saw intracellular bacteria infrequently in the mosquito gut, suggesting there were intrinsic factors limiting the systemic infection. Innate immunity may be respsonsible for maintaining homeostatsis, which would be consistent with our gene expression data, or alternatively, these mutualistic bacteria may exploit similar molecular processes as their pathogenic counterparts to overcome host immune pathways [74]. The intracellular lifestyle of bacteria and their ability to egress from cells likely facilitates microbial persistence in these holometabolous insects. Our finding of intracellular bacteria in the malpighian tubules further supports this theory as bacteria residing within this tissue are known to be transstadially transmitted [4].

Conclusions

346 In conclusion, we have shown through various *in vitro* and *in vivo* data that symbiotic
347 *Enterobacteriaceae* can invade and replicate intracellularly in mosquito cells. Bacterial
348 invasion is mediated by host actin filaments and beta-integrin receptors. Intracellular
349 bacteria dramatically upregulate host IMD and Toll immune pathways and substantially
350 reduce ZIKV density in cells. These data enhance our understanding of host-microbe
351 interactions in mosquitoes and point to a possible mechanism by which bacteria, which
352 are commonly associated with the midgut, could infect other tissues within mosquitoes.
353
354 **Material and Methods.**
355 **Ethics statement:** ZIKV, which was originally isolated from an *Ae. aegypti* mosquito
356 (Chiapas State, Mexico), was obtained from the World Reference Center for Emerging
357 Viruses and Arboviruses at the University of Texas Medical Branch (Galveston, TX).
358 Experimental work with the virus was approved by the University of Texas Medical
359 Branch Institutional Biosafety Committee (reference number 2016055).
360
361 **Isolation of bacteria from mosquitoes:** Lab reared *Ae. albopictus* mosquitoes were
362 collected and surface sterilized before homogenized in 500 µl of 1X PBS. Serial dilution
363 of homogenates was plated on LB agar plate to obtain isolated colonies. The single
364 colonies were picked, grown in LB medium before isolating genomic DNA. The 16S
365 rDNA PCR was performed as described previously [75] and the PCR product was
366 Sanger sequenced to identify the bacterial species. To further classify the gut-
367 associated bacteria we completed multilocus sequence typing (MLST) as described
368 previously [11, 76]. The MLST sequences were aligned, concatenated and a maximum

likelihood tree under the LG model and rapid bootstrap was constructed using Seaview [77] (Fig. S6). The sequences have been deposited under accession numbers XXXX.

Bacterial growth and cell culture: Two bacterial isolates were grown in LB medium at 37°C. The overnight culture was appropriately diluted in Schneider's media (Gibco) to obtain the MOI of 10 before the infection. The mosquito cell lines were maintained in their respective medium at 28 °C. The *Ae. aegypti* cell line Aag2 [78] and Sua5B cells were maintained in *Drosophila* Schneider's medium (Gibco) supplemented with 20% FBS (Denville Scientific) and 1% penicillin/streptomycin (P/S; 100 Units/mL and 100 µg/mL respectively), RML-12 cells were maintained in Leibovitz' (L15) medium (Gibco) containing 20% FBS and 10% tryptose phosphate broth. Vero cells (CCL-81) were purchased from the American Type Culture Collection (Bethesda, MD, USA) and maintained in DMEM supplemented with 5% FBS and 1% P/S (100 Units/mL and 100 µg/mL respectively) at 37 °C with 5% CO_2.

Gentamicin invasion assay: The gentamicin invasion assay was performed as described elsewhere with minor alterations [33]. Aag2 cells were seeded at the density of $1x10^5$/well in 24-well plate 48h prior to infection. On the day of infection, cells were washed in Schneider's media (Gibco) and infected with 500 µl of bacterial suspension. After incubating for 1h at 28 °C, bacteria were removed, and cells were washed once with Schneider's medium and incubated with 200 µg/ml gentamicin for additional 1h to kill extracellular bacteria. The invaded bacteria were recovered after washing the cells

391 twice with Schneider's media and lysing them in 500 µl of 1X PBS containing 0.05%
392 Triton X-100.
393
394 **Fluorescence and Transmission electron microscopy:** In order to assess the
395 invasion of symbionts fluorescent microscopy and TEM was performed on the Aag2
396 cells after allowing bacteria to invade. The bacteria were transformed with mCherry
397 expressing plasmid pRAM18dRGA-mCherry, which is a modified version of
398 pRAM18dRGA[MCS] [41]. Aag2 cells were fixed with 1% PFA (Electron Microscopy
399 Sciences, Hartfield, PA) for 30 min and permeabilized in 1X PBS+0.01 % Triton X-100
400 (Fischer Scientific) for 20 min following staining with Atto 488 Phalloidin (Sigma) as per
401 manufacturers recommendations. The cell nuclei were stained with DAPI after washing
402 the slides in 1X PBS. The slides were stored in Prolong-Antifade (Invitrogen). The
403 samples were observed using the Revolve-FL epifluorescence microscope (ECHOLAB).
404 For TEM, insect cells were fixed in fixative (2.5% formaldehyde, 0.1% glutaraldehyde,
405 0.03% picric acid, 0.03% $CaCl_2$ and 0.05 M cacodylate buffer at pH 7.3) and post fixed
406 in 1% osmium tetroxide for 1 h, stained *en bloc* in 2% aqueous uranyl acetate at 60 °C
407 for 20 min, dehydrated in a graded series of ethanol concentrations, and embedded in
408 epoxy resin, Poly/Bed 812. Ultrathin sections were cut on a Leica EM UC7 (Leica
409 Microsystems, Buffalo Grove, IL), placed on Formvar-carbon copper 200 mesh grids,
410 stained with lead citrate and examined in a Philips (FEI) CM-100 electron microscope at
411 60 kV. To assess the *in vivo* invasion in mosquito larvae and adults, guts were
412 dissected after surface sterilization in 1X PBS and then the tissue was fixed in fixative
413 (2.5% glutaraldehyde and 2% paraformaldehyde buffered with 0.1 M sodium

cacodylate) for 2 hours and post fixed in 1% osmium tetroxide for 1 h at room temperature. Then samples were dehydrated in a graded series of ethanol concentrations, and embedded in epoxy resin, Epon 812. The sections were prepared as described above and imaged in a Tecnai Spirit (FEI) transmission electron microscope at 80 kV. For Confocal Laser Scanning Microscopy, tissue samples were fixed in 1% PFA in 1X PBS for 30 min, then permebalized with 0.01% Triton X-100 in 1X PBS for 20 min before staining with SiR-actin Kit (Spirochrome AG, Switzerland) for 1 hour and DAPI (Applied Biosystems) for 15 min. Then tissue samples were embedded in 1% low-melting agarose with SlowFade Diamond mounting solution (Molecular Probes). Samples were imaged and 3D-reconstructed (1.3 mm sections) using a Zeiss LSM-800 and were analysed in Zen 3.0 (Zeiss) and Fiji (ImageJ).

Intracellular replication of *Cedecea neteri*: To assess the replication of bacteria inside the host cells as well as in the medium, the Aag2 cells innoculated with *C. neteri* were incubated with or without gentamicin for 8h at 28 °C. Every two hours, the supernatant was collected and serial dilutions were plated on LB agar plate to enumerate the bacterial quantity in the medium. The cells were washed two times with Schneider's medium before plating on agar plate.

Host cytoskeleton and Janus Kinase in *Cedecea neteri* invasion: The gentamicin invasion assay was performed in the presence of actin and Janus kinase (JAK) inhibitors. The assay was performed by pre-incubating Aag2 cells in presence of 10 or 20 μg/ml of Cytochalasin D (Sigma) and 30 or 60 μg/ml of Sp600125 (Sigma) for 1 hr.

437 The gentamicin invasion assay was performed as described above with the addition of
438 each specific drug. A 60 μg/ml of DMSO treatment was used as a control.
439
440 **RNAi mediated integrin gene silencing in Aag2 cells:** In order to assess the role of
441 host integrin receptors in the invasion of *C. neteri*, the integrin alpha and beta receptors
442 were depleted using RNAi. dsRNA was designed for AAEL001829 and AAEL014660
443 using E-RNAi [79] and amplified using primers with flanking T7 promoter sequence
444 using *Ae. aegypti* cDNA as a template. dsRNA was synthesized using the T7
445 megascript kit (Ambion). The primers are listed in the Table S1. dsDNA against GFP
446 was used as control. Aag2 cells were transfected with 0.5 μg of each dsRNA using
447 Lipofectamine™ RNAiMAX (Life Technologies) 48hrs prior to bacterial infection and the
448 gentamicin invasion assay.
449
450 **RT-qPCR analysis:** Total RNA was isolated from Aag2 cells and reverse transcribed
451 using the amfiRivert cDNA synthesis Platinum master mix (GenDepot, Barker, TX, USA)
452 containing a mixture of oligo(dT)18 and random hexamers. Real-time quantification was
453 performed in a StepOnePlus instrument (Applied Biosystems, Foster City, CA) in a 10 μl
454 reaction mixture containing 10-20 ng cDNA template, 1X PowerUp SYBR green master
455 mix (Applied Biosystems), and 1 μM (each) primer. The analysis was performed using
456 the threshold cycle (ΔΔ CT) (Livak) method [80]. Four independent biological replicates
457 were conducted, and all PCRs were performed in duplicate. In order to assess the
458 expression of innate immune genes, the invasion assay was performed as described
459 earlier and post 24-hr invasion cells were harvested to isolate RNA, followed by cDNA

460 synthesis and RT-qPCR for specific genes. The ribosomal protein S7 gene [81] was
461 used for normalization of cDNA templates. Primer sequences are listed in Table S1.
462
463 ***In vitro* vector competence of ZIKV in Aag2 cells:** The assay was performed in order
464 to assess the how intracellular bacteria modulate ZIKV infection *in vitro*. After the
465 gentamicin invasion assay with *C. neteri* at an MOI of 1:1, 1:2, 1:5 and 1:10. After 24
466 hrs, the supernatant was removed, and cells were washed twice with 1x PBS before
467 infecting with ZIKV (Mex 1-7 strain) [82] at an MOI of 1:0.1. After 4 days, supernatant
468 was collected and ZIKV was quantified by focus forming assay [82]. The experiment
469 was repeated three times.
470 **Gnotobiotic rearing and *in vivo* invasion in mosquitoes:** *Ae. aegypti* gnotobiotic
471 larvae were generated as previously described [83]. To synchronize hatching, sterile
472 eggs were transferred to a conical flask and placed under a vacuum for 45 min. To
473 verify sterility, larval water was plated on non-selective LB agar plates. Twenty L1 larvae
474 were transferred to a T75 tissue culture flask and inoculated with transgenic symbionts
475 possessing the pRAM18dRGA-mCherry at $1x10^7$. Bacterial cultures were quantified with
476 a spectrophotometer (DeNovix DS-11, DeNovix) and validated by plating and
477 determining colony forming units. L1 larvae grown without bacteria were used as
478 contamination control, and these mosquitoes did not reach pupation [83]. To feed
479 mosquitoes, ground fish food pellets were sterilized by autoclaving and then mixed with
480 sterile water. 60 µl of fish food (1 µg/µl) was fed to larvae on alternative days.
481
482 **Acknowledgements.**

We would like to thank the UTMB insectary core for providing the lab mosquitoes. GLH is supported by NIH grants (R21AI138074, R21AI124452 and R21AI129507), the Wolfson Foundation and Royal Society (RSWF\R1\180013), the John S. Dunn Foundation Collaborative Research Award, and the Centers for Disease Control and Prevention (Cooperative Agreement Number U01CK000512). The paper contents are solely the responsibility of the authors and do not necessarily represent the official views of the Centers for Disease Control and Prevention or the Department of Health and Human Services. This work was also supported by a James W. McLaughlin postdoctoral fellowship at the University of Texas Medical Branch to SH and a NIH T32 fellowship (2T32AI007526) to MAS and Anti-VeC AV/PP0021//1 to AAS. Microscopy core facility at NYBC was supported by NYBC intramural fund. Confocal imaging facilities were funded by a Wellcome Trust Multi-User Equipment Grant (104936/Z/14/Z).

Author Contributions

SH and GLH designed the experiments. SH, DV, ACS, MAS, and VLP completed the experiments. SH, DV, VLP, AKC, and GLH undertook analysis. SH, AKC, AAS, and GLH wrote and edited the manuscript and all authors agreed to the final version. GLH acquired the funding and supervised the work.

Figure legends

Figure 1. Invasion of symbiotic bacteria into mosquito cells. The gentamicin invasion assay was used to examine the invasive capacity of symbiotic *Enterobacteriaceae* bacteria isolated from *Aedes* mosquitoes (A). Non-invasive *E. coli* was used as negative control. *E. coli* expressing the *Yersinia inv (Ypinv)* gene was used as a positive control. The assay was repeated twice. Flourscent and transmission electron microscopy was used to visual intracellular bacteria (B). Bacteria expressed mCherry fluorescent protein (red), actin filaments were stained with Phalloidin (green) and DNA with DAPI (blue). Arrowheads in the TEM images indicate vacuoles containing bacteria. Scale bar is 500 nm. Density (C) and time dependent (D) invasion of *C. neteri* in Aag2 cells. The density dependant invasion assay (C) was replicated twice. The time dependant invasion assay was done at host cell: bacterial density of 1:10 (N=4). *C. neteri* invasion in *Aedes aegypti (*Aag2 and RML-12) *and Anopheles gambiae* (Sua5B) (E). The assay was repeated twice. Letters indicate significant differences ($p < 0.05$) determined by a One-Way ANOVA with a Tukey's multiple comparison test.

Figure 2. Intracellular replication and egression of *C. neteri* in Aag2 cells. TEM of Aag2 cells containing invaded *C. neteri* replicating inside Aag2 cell (A). Arrow indicates the dividing bacterial cell. Bacterial titer in cells (B) or in the cell culture media (C) in the presence and absence of gentamicin. The significance between the gentamicin and non-treated samples at different time post invasion was analyzed by Unpaired t test. Five replicates were used at each time point.

Figure 3. The role of host cytoskeletal proteins and receptors in the *C. neteri* invasion. Invasion of *C. neteri* in the presence of inhibotors of actin polymerisation (Cyt D) and phagocytosis (SP600125 [Sp]) (A). DMSO was used as control to assess its cytotoxic effect on the cells. *C. neteri* invasion after silencing of the beta- (B) and alpha- (C) integrins. The expeirments were repeated twice. Letters indicate significant differences ($p < 0.05$) determined by a One-Way ANOVA with a Tukey's multiple comparison test.

Figure 4. Intracellular bacteria reduces ZIKV titer in *Ae. aegypti* cells. ZIKV infection at 2 (A) and 4 (B) days post invasion compared to an uninfected control. ZIKV infection in *C. neteri* or *Serratia* sp. infected cells (C). The effect of bacterial density on ZIKV infection (D). *C. neteri* and *E. coli* were inoculated onto cells using the gentamicin invasion assay at increasing MOIs. For the *C. neteri* 1:2, 1:5, and 1:10 and *E. coli* 1:10 treatments, no ZIKV was recovered from cells. For A, B and D significance was determind using unpaired t-test, while for C, significance was calculated by one-way ANNOVA with Tukey's multiple comparison test.

Figure 5. Intracellular *C. neteri* upregulates mosquito Toll and IMD innate immune pathways. Gene expression analysis of the NF-κB transcriptional activators (A) and the negative regulators (B) of the Toll, IMD and JAK-STAT pathways as well as downstream effector molecules (C). Gene expression was measured 24 hr post *C. neteri* invasion in Aag2 cells. Gene expression of the NF-κB transcriptional activators (D) and the negative regulators (E) in cells co-infected with *C. neteri* or *Serratia* sp. and

ZIKV. 24 hours post bacterial infection cells were infected with ZIKV. Samples were collected 4 days post ZIKV infection for qPCR analysis. The experiment was repeated twice. Letters indicate significant differences ($p < 0.05$) determined by a One-Way ANOVA with a Tukey's multiple comparison test.

Figure 6. Intracellular localization of *Cedecea* and *Serratia* in mosquito tissues. TEM micrographs of *Serratia* sp. (Sm) accumulated in the gut lumen and associated with the microvilli of the gut epithelium in mono-axenically infected *Ae. aegypti* adults (A). Magnified image of bacteria attaching to microvilli (MV) (B), and bacteria in the process of entering or exiting the gut epithelia (purple and green insert). (B) Intracellular *C. neteri* (Cn) in the larval gut mono-axenically infected *Ae. aegypti*. Mitochondria (M) and nucleus (N). Yellow and blue inserts show larger view of bacteria from B. CLSM evidence of the intracellular localization of *C. neteri* in the adult mosquito gut and Malpighian tubules (C). Bright field (left) and maximum intensity projection (right) of tissues 3D-reconstructed from a series of Z-stacks merging mosquito actin (white), mCherry-expressing *C. neteri* (yellow) and DAPI-stained DNA (magenta). Two representative XZ and YZ orthogonal views (OV1-4) of the stacks are shown for each tissue on the sides, and the identity of intracellular bacteria examples is noted with colored squares. On the right, the plots coloured according to the identity of the corresponding bacterium, show the co-localization of the actin signal (gray) with the mCherry bacteria (yellow). Scale bars are 50 μm.

Supplementary figure legends

Figure S1. Gentamicin invasion assay in different cell lines. Invasion of *E. coli* and *E. coli BL21* expressing the *Yersina invasion* gene (*Ypinv*) in different cell lines. The assay was done in Aag2 (*Aedes aegypti*), Sua5B (*Anopheles gambiae*) and Vero (Monkey kidney cells). The assay was done twice. The statistical significance was determined using an Unpaired t-test.

Figure S2. Flourscent microscopy of bacteria in Aag2 cells. Merged and separate channels – blue (DAPI), green (actin filaments stained with Phalloidin), red (bacteria expressing mCherry). Scale bars are 70 μm.

Figure S3. Effect of intracellular bacteria on the cell viability. Aag2 cell numbers at different times post invasion with *C. neteri.* Cells were supplement with gentamicin (200 μg/ml) or cultured in the absence of antibiotic.

Figure S4. Validation of gene silencing in cells. RT-qPCR analysis of beta (A) and alpha (B) integrin gene expression 24 hours post transfection of dsRNA. dsRNAs targetting GFP were used as the negative control. The experiment was repeated twice. The statistical significance was determined using an Unpaired t-test.

Figure S5. CLSM analyses of infected adult gut and Malpighian tubule. Maximum intensity projection of tissues 3D-reconstructed from a series of Z-stacks merging mosquito actin (white), mCherry-expressing *Cedecea* (yellow) and DAPI-stained DNA

(magenta). Several XZ and YZ orthogonal views (OV) of the stacks are shown for each tissue on the sides. Scale bars are 50 μm.

Figure S6. Phylogenetic analysis of multilocus sequence typing as described in [76] shows the phylogenetic position of *Serratia sp.* Alb1 (in red; this study) and *C. neteri* Alb1 (in blue; [11]). The tree analysis was performed using PhyML under the general time-reversible model with rapid aLRT bootstrap support as implemented as default in seaview (v4.7; [77]. The *Serratia* sp. Alb1 sequences were submitted to NCBI under accession numbers XXX (ropB), XXX (gyrB), XXX (atpD) and XXX (infB). [Accession numbers requested and will be updated in revision process as soon as available].

Supporting files.

Supporting file S1. Tree file, including all support values.

Supplementary table legends.

Table S1. Primer sequences used in this study

Supplementary video legends.

Video S1. Series of Z-stacks of an adult infected gut by CLSM.

Video S2. Series of Z-stacks of an adult infected Malpighian tubule by CLSM.

618 **Reference:**

619

620 1. Duguma D, Hall MW, Smartt CT, Neufeld JD. Effects of Organic Amendments on
621 Microbiota Associated with the Culex nigripalpus Mosquito Vector of the Saint Louis
622 Encephalitis and West Nile Viruses. mSphere. 2017;2(1). Epub 2017/02/09. doi:
623 10.1128/mSphere.00387-16.
624 2. Dada N, Jumas-Bilak E, Manguin S, Seidu R, Stenström T-A, Overgaard HJ.
625 Comparative assessment of the bacterial communities associated with Aedes aegypti
626 larvae and water from domestic water storage containers. Parasites &
627 Vectors. 2014;7(1):391. doi: 10.1186/1756-3305-7-391.
628 3. Gusmao DS, Santos AV, Marini DC, Russo Ede S, Peixoto AM, Bacci Junior M,
629 et al. First isolation of microorganisms from the gut diverticulum of Aedes aegypti
630 (Diptera: Culicidae): new perspectives for an insect-bacteria association. Mem Inst
631 Oswaldo Cruz. 2007;102(8):919-24. Epub 2008/01/23. doi: 10.1590/s0074-
632 02762007000800005.
633 4. Chavshin AR, Oshaghi MA, Vatandoost H, Yakhchali B, Zarenejad F, Terenius
634 O. Malpighian tubules are important determinants of Pseudomonas transstadial
635 transmission and longtime persistence in Anopheles stephensi. Parasites &
636 Vectors. 2015;8(1):36. doi: 10.1186/s13071-015-0635-6.
637 5. Chen S, Bagdasarian M, Walker ED. *Elizabethkingia anophelis*: Molecular
638 Manipulation and Interactions with Mosquito Hosts. Applied and Environmental
639 Microbiology. 2015;81(6):2233. doi: 10.1128/AEM.03733-14.

640 6. Alonso DP, Mancini MV, Damiani C, Cappelli A, Ricci I, Alvarez MVN, et al.
641 Genome Reduction in the Mosquito Symbiont Asaia. Genome Biol Evol. 2019;11(1):1-
642 10. Epub 2018/11/27. doi: 10.1093/gbe/evy255.
643 7. Duguma D, Hall MW, Smartt CT, Debboun M, Neufeld JD. Microbiota variations
644 in Culex nigripalpus disease vector mosquito of West Nile virus and Saint Louis
645 Encephalitis from different geographic origins. PeerJ. 2019;6:e6168. Epub 2019/01/16.
646 doi: 10.7717/peerj.6168.
647 8. Osei-Poku J, Mbogo CM, Palmer WJ, Jiggins FM. Deep sequencing reveals
648 extensive variation in the gut microbiota of wild mosquitoes from Kenya. Molecular
649 Ecology. 2012;21(20):5138-50. doi: 10.1111/j.1365-294X.2012.05759.x.
650 9. Muturi EJ, Ramirez JL, Rooney AP, Kim C-H. Comparative analysis of gut
651 microbiota of mosquito communities in central Illinois. PLoS Neglected Tropical
652 Diseases. 2017;11(2):e0005377-18. doi: 10.1371/journal.pntd.0005377.
653 10. Pei D, Jiang J, Yu W, Kukutla P, Uentillie A, Xu J. The *waaL* gene mutation
654 compromised the inhabitation of *Enterobacter sp. Ag1* in the mosquito gut environment.
655 Parasites & Vectors. 2015:1-10. doi: 10.1186/s13071-015-1049-1.
656 11. Hegde S, Nilyanimit P, Kozlova E, Anderson ER, Narra HP, Sahni SK, et al.
657 CRISPR/Cas9-mediated gene deletion of the ompA gene in symbiotic Cedecea neteri
658 impairs biofilm formation and reduces gut colonization of Aedes aegypti mosquitoes.
659 PLOS Neglected Tropical Diseases. 2019;13(12):e0007883. doi:
660 10.1371/journal.pntd.0007883.

661 12. Guegan M, Zouache K, Demichel C, Minard G, Tran Van V, Potier P, et al. The
662 mosquito holobiont: fresh insight into mosquito-microbiota interactions. Microbiome.
663 2018;6(1):49. Epub 2018/03/21. doi: 10.1186/s40168-018-0435-2.
664 13. Brady OJ, Godfray HC, Tatem AJ, Gething PW, Cohen JM, McKenzie FE, et al.
665 Vectorial capacity and vector control: reconsidering sensitivity to parameters for malaria
666 elimination. Trans R Soc Trop Med Hyg. 2016;110(2):107-17. Epub 2016/01/30. doi:
667 10.1093/trstmh/trv113.
668 14. Hegde S, Rasgon JL, Hughes GL. The microbiome modulates arbovirus
669 transmissionin mosquitoes. Current Opinion in Virology. 2015;15:97-102. doi:
670 10.1016/j.coviro.2015.08.011.
671 15. Caragata EP, Tikhe CV, Dimopoulos G. Curious entanglements: interactions
672 between mosquitoes, their microbiota, and arboviruses. Current Opinion in Virology.
673 2019;37:26-36. doi: https://doi.org/10.1016/j.coviro.2019.05.005.
674 16. Saldaña MA, Hegde S, Hughes GL. Microbial control of arthropod-borne disease.
675 Memórias do Instituto Oswaldo Cruz. 2017;112(2):81-93. doi: 10.1590/0074-
676 02760160373.
677 17. Ricci I, Damiani C, Capone A, DeFreece C, Rossi P, Favia G.
678 Mosquito/microbiota interactions: from complex relationships to biotechnological
679 perspectives. Current Opinion in Microbiology. 2012;15(3):278-84. doi:
680 10.1016/j.mib.2012.03.004.
681 18. Berhanu A, Abera A, Nega D, Mekasha S, Fentaw S, Assefa A, et al. Isolation
682 and identification of microflora from the midgut and salivary glands of Anopheles

683 species in malaria endemic areas of Ethiopia. BMC Microbiol. 2019;19(1):85. Epub
684 2019/05/01. doi: 10.1186/s12866-019-1456-0.
685 19. Dickson LB, Ghozlane A, Volant S, Bouchier C, Ma L, Vega-Rua A, et al. Diverse
686 laboratory colonies of Aedes aegypti harbor the same adult midgut bacterial
687 microbiome. Parasites & Vectors. 2018;11(1):207. doi: 10.1186/s13071-018-
688 2780-1.
689 20. Damiani C, Ricci I, Crotti E, Rossi P, Rizzi A, Scuppa P, et al. Paternal
690 transmission of symbiotic bacteria in malaria vectors. Current biology : CB.
691 2008;18(23):R1087-8. doi: 10.1016/j.cub.2008.10.040.
692 21. Sharma P, Sharma S, Maurya RK, Das De T, Thomas T, Lata S, et al. Salivary
693 glands harbor more diverse microbial communities than gut in Anopheles culicifacies.
694 Parasites & Vectors. 2014;7(1):235. doi: 10.1186/1756-3305-7-235.
695 22. Gimonneau G, Tchioffo MT, Abate L, Boissière A, Awono-Ambene PH, Nsango
696 SE, et al. Composition of Anopheles coluzzii and Anopheles gambiae microbiota from
697 larval to adult stages. Infection, genetics and evolution : journal of molecular
698 epidemiology and evolutionary genetics in infectious diseases. 2014;28:715-24. doi:
699 10.1016/j.meegid.2014.09.029.
700 23. Mancini MV, Damiani C, Accoti A, Tallarita M, Nunzi E, Cappelli A, et al.
701 Estimating bacteria diversity in different organs of nine species of mosquito by next
702 generation sequencing. BMC Microbiol. 2018;18(1):126. Epub 2018/10/06. doi:
703 10.1186/s12866-018-1266-9.
704 24. Segata N, Baldini F, Pompon J, Garrett WS, Truong DT, Dabiré RK, et al. The
705 reproductive tracts of two malaria vectors are populated by a core microbiome and by

706 gender- and swarm-enriched microbial biomarkers. Scientific Reports. 2016;6:24207.
707 doi: 10.1038/srep24207.
708 25. Tchioffo MT, Boissiere A, Abate L, Nsango SE, Bayibeki AN, Awono-Ambene
709 PH, et al. Dynamics of Bacterial Community Composition in the Malaria Mosquito's
710 Epithelia. Front Microbiol. 2015;6:1500. Epub 2016/01/19. doi:
711 10.3389/fmicb.2015.01500.
712 26. Koosha M, Vatandoost H, Karimian F, Choubdar N, Oshaghi MA. Delivery of a
713 Genetically Marked Serratia AS1 to Medically Important Arthropods for Use in RNAi and
714 Paratransgenic Control Strategies. Microb Ecol. 2018. Epub 2018/11/22. doi:
715 10.1007/s00248-018-1289-7.
716 27. Wang S, Dos-Santos ALA, Huang W, Liu KC, Oshaghi MA, Wei G, et al. Driving
717 mosquito refractoriness to *Plasmodium falciparum* with engineered symbiotic bacteria.
718 Science (New York, NY). 2017;357(6358):1399-402. doi: 10.1126/science.aan5478.
719 28. Damiani C, Ricci I, Crotti E, Rossi P, Rizzi A, Scuppa P, et al. Mosquito-Bacteria
720 Symbiosis: The Case of Anopheles gambiae and Asaia. Microb Ecol. 2010;60(3):644-
721 54. doi: 10.1007/s00248-010-9704-8.
722 29. Wei G, Lai Y, Wang G, Chen H, Li F, Wang S. Insect pathogenic fungus interacts
723 with the gut microbiota to accelerate mosquito mortality. Proceedings of the National
724 Academy of Sciences of the United States of America. 2017;114(23):5994-9. doi:
725 10.1073/pnas.1703546114.
726 30. Nehme NT, Liégeois S, Kele B, Giammarinaro P, Pradel E, Hoffmann JA, et al. A
727 model of bacterial intestinal infections in Drosophila melanogaster. 2007;3(11):e173.
728 doi: 10.1371/journal.ppat.0030173.

729 31. Czuczman MA, Fattouh R, van Rijn JM, Canadien V, Osborne S, Muise AM, et
730 al. Listeria monocytogenes exploits efferocytosis to promote cell-to-cell spread. Nature.
731 2014;509(7499):230-4. Epub 2014/04/18. doi: 10.1038/nature13168.
732 32. Ribet D, Cossart P. How bacterial pathogens colonize their hosts and invade
733 deeper tissues. Microbes and infection. 2015;17(3):173-83. doi:
734 10.1016/j.micinf.2015.01.004.
735 33. Hegde S, Hegde S, Spergser J, Brunthaler R, Rosengarten R, Chopra-
736 Dewasthaly R. In vitro and in vivo cell invasion and systemic spreading of Mycoplasma
737 agalactiae in the sheep infection model. International journal of medical microbiology :
738 IJMM. 2014;304(8):1024-31. doi: 10.1016/j.ijmm.2014.07.011.
739 34. Tchioffo MT, Abate L, Boissière A, Nsango SE, Gimonneau G, Berry A, et al. An
740 epidemiologically successful Escherichia coli sequence type modulates Plasmodium
741 falciparum infection in the mosquito midgut. Infection, genetics and evolution : journal of
742 molecular epidemiology and evolutionary genetics in infectious diseases. 2016;43:22-
743 30. doi: 10.1016/j.meegid.2016.05.002.
744 35. Elsinghorst EA. Measurement of invasion by gentamicin resistance. Methods
745 Enzymol. 1994;236:405-20. Epub 1994/01/01.
746 36. Isberg RR, Falkow S. A single genetic locus encoded by Yersinia
747 pseudotuberculosis permits invasion of cultured animal cells by Escherichia coli K-12.
748 Nature. 1985;317(6034):262-4.
749 37. Isberg RR, Voorhis DL, Falkow S. Identification of invasin: a protein that allows
750 enteric bacteria to penetrate cultured mammalian cells. Cell. 1987;50(5):769-78. Epub
751 1987/08/28. doi: 10.1016/0092-8674(87)90335-7.

752 38. Dersch P, Isberg RR. A region of the Yersinia pseudotuberculosis invasin protein
753 enhances integrin-mediated uptake into mammalian cells and promotes self-
754 association. The EMBO Journal. 1999;18(5):1199-213. doi: 10.1093/emboj/18.5.1199.
755 39. Trujillo-Ocampo A, Cazares-Raga FE, Del Angel RM, Medina-Ramirez F,
756 Santos-Argumedo L, Rodriguez MH, et al. Participation of 14-3-3epsilon and 14-3-3zeta
757 proteins in the phagocytosis, component of cellular immune response, in Aedes
758 mosquito cell lines. Parasit Vectors. 2017;10(1):362. Epub 2017/08/03. doi:
759 10.1186/s13071-017-2267-5.
760 40. Dimopoulos G, Müller HM, Levashina EA, Kafatos FC. Innate immune defense
761 against malaria infection in the mosquito. Current Opinion in Immunology.
762 2001;13(1):79-88.
763 41. Hegde S, Khanipov K, Albayrak L, Golovko G, Pimenova M, Saldaña MA, et al.
764 Microbiome interaction networks and community structure from laboratory-reared and
765 field-collected *Aedes aegypti*, *Aedes albopictus*, and *Culex quinquefasciatus* mosquito
766 vectors. Frontiers in Microbiology. 2018;9:715. doi: 10.3389/fmicb.2018.02160.
767 42. Gupta L, Molina-Cruz A, Kumar S, Rodrigues J, Dixit R, Zamora RE, et al. The
768 STAT pathway mediates late-phase immunity against Plasmodium in the mosquito
769 Anopheles gambiae. Cell Host & Microbe. 2009;5(5):498-507. doi:
770 10.1016/j.chom.2009.04.003.
771 43. Wright JD, Barr AR. The ultrastructure and symbiotic relationships of Wolbachia
772 of mosquitoes of the Aedes scutellaris group. Journal of Ultrastructure Research.
773 1980;72(1):52-64. doi: https://doi.org/10.1016/S0022-5320(80)90135-5.

774 44. Fattouh N, Cazevieille C, Landmann F. Wolbachia endosymbionts subvert the
775 endoplasmic reticulum to acquire host membranes without triggering ER stress. PLOS
776 Neglected Tropical Diseases. 2019;13(3):e0007218. doi: 10.1371/journal.pntd.0007218.
777 45. Traven A, Naderer T. Microbial egress: a hitchhiker guide to freedom. PLOS
778 Pathogens. 2014;10(7):e1004201. doi: 10.1371/journal.ppat.1004201.
779 46. Flieger A, Frischknecht F, Hacker G, Hornef MW, Pradel G. Pathways of host cell
780 exit by intracellular pathogens. Microb Cell. 2018;5(12):525-44. Epub 2018/12/12. doi:
781 10.15698/mic2018.12.659.
782 47. Haglund CM, Welch MD. Pathogens and polymers: microbe-host interactions
783 illuminate the cytoskeleton. J Cell Biol. 2011;195(1):7-17. Epub 2011/10/05. doi:
784 10.1083/jcb.201103148.
785 48. Hybiske K, Stephens R. Cellular Exit Strategies of Intracellular Bacteria.
786 Microbiol Spectr. 2015;3(6). Epub 2016/06/24. doi: 10.1128/microbiolspec.VMBF-0002-
787 2014.
788 49. Fukumatsu M, Ogawa M, Arakawa S, Suzuki M, Nakayama K, Shimizu S, et al.
789 Shigella targets epithelial tricellular junctions and uses a noncanonical clathrin-
790 dependent endocytic pathway to spread between cells. Cell Host & Microbe.
791 2012;11(4):325-36. doi: 10.1016/j.chom.2012.03.001.
792 50. Casella JF, Flanagan MD, Lin S. Cytochalasin D inhibits actin polymerization and
793 induces depolymerization of actin filaments formed during platelet shape change.
794 Nature. 1981;293(5830):302-5. Epub 1981/09/24. doi: 10.1038/293302a0.
795 51. Mizutani T, Kobayashi M, Eshita Y, Shirato K, Kimura T, Ako Y, et al.
796 Involvement of the JNK-like protein of the Aedes albopictus mosquito cell line, C6/36, in

797 phagocytosis, endocytosis and infection of West Nile virus. Insect Mol Biol. 2003;12.
798 doi: 10.1046/j.1365-2583.2003.00435.x.
799 52. Lin M, Kikuchi T, Brewer HM, Norbeck AD, Rikihisa Y. Global Proteomic Analysis
800 of Two Tick-Borne Emerging Zoonotic Agents: Anaplasma Phagocytophilum and
801 Ehrlichia Chaffeensis. Frontiers in Microbiology. 2011;2. doi:
802 10.3389/fmicb.2011.00024.
803 53. Martinez JJ, Cossart P. Early signaling events involved in the entry of Rickettsia
804 conorii into mammalian cells. Journal Of Cell Science. 2004;117(Pt 21):5097-106. doi:
805 10.1242/jcs.01382.
806 54. Wesolowski J, Paumet F. Taking control: reorganization of the host cytoskeleton
807 byChlamydia. F1000Research. 2017;6:2058. doi: 10.12688/f1000research.12316.1.
808 55. Moita L, Vriend G, Mahairaki V, Louis C, Kafatos F. Integrins of Anopheles
809 gambiae and a putative role of a new β integrin, BINT2, in phagocytosis of E. coli. Insect
810 Biochemistry and Molecular Biology. 2006;36(4):282-90. doi:
811 10.1016/j.ibmb.2006.01.004.
812 56. Eto DS, Jones TA, Sundsbak JL, Mulvey MA. Integrin-mediated host cell
813 invasion by type 1-piliated uropathogenic Escherichia coli. PLOS Pathogens.
814 2007;3(7):e100. doi: 10.1371/journal.ppat.0030100.
815 57. Wu J, Weening EH, Faske JB, Höök M, Skare JT. Invasion of Eukaryotic Cells by
816 Borrelia burgdorferiRequires β 1Integrins and Src Kinase Activity. Infection and
817 Immunity. 2011;79(3):1338-48. doi: 10.1128/IAI.01188-10.

818 58. Gillenius E, Urban CF. The adhesive protein invasin of Yersinia
819 pseudotuberculosis induces neutrophil extracellular traps via β1 integrins. Microbes and
820 infection. 2015;17(5):327-36. doi: 10.1016/j.micinf.2014.12.014.
821 59. Miesen P, van Rij RP. Crossing the Mucosal Barrier: A Commensal Bacterium
822 Gives Dengue Virus a Leg-Up in the Mosquito Midgut. Cell Host Microbe. 2019;25(1):1-
823 2. Epub 2019/01/11. doi: 10.1016/j.chom.2018.12.009.
824 60. Coatsworth H, Caicedo PA, Van Rossum T, Ocampo CB, Lowenberger C. The
825 Composition of Midgut Bacteria in Aedes aegypti (Diptera: Culicidae) That Are Naturally
826 Susceptible or Refractory to Dengue Viruses. Journal of Insect Science. 2018;18(6).
827 doi: 10.1093/jisesa/iey118.
828 61. Hegde S, Hegde S, Hegde S, Zimmermann M, Flöck M, Spergser J, et al.
829 Simultaneous Identification of Potential Pathogenicity Factors of Mycoplasma agalactiae
830 in the Natural Ovine Host by Negative Selection. Infection and Immunity.
831 2015;83(7):2751-61. doi: 10.1128/IAI.00403-15.
832 62. Broderick NA. Friend, foe or food? Recognition and the role of antimicrobial
833 peptides in gut immunity and Drosophila-microbe interactions. Philosophical
834 transactions of the Royal Society of London Series B, Biological sciences.
835 2016;371(1695):20150295. doi: 10.1098/rstb.2015.0295.
836 63. Buchon N, Broderick NA, Poidevin M, Pradervand S, Lemaitre B. Drosophila
837 intestinal response to bacterial infection: activation of host defense and stem cell
838 proliferation. Cell Host & Microbe. 2009;5(2):200-11. doi:
839 10.1016/j.chom.2009.01.003.

840 64. Cheng G, Liu Y, Wang P, Xiao X. Mosquito Defense Strategies against Viral
841 Infection. Trends Parasitol. 2016;32(3):177-86. Epub 2015/12/03. doi:
842 10.1016/j.pt.2015.09.009.
843 65. Fragkoudis R, Attarzadeh-Yazdi G, Nash AA, Fazakerley JK, Kohl A. Advances
844 in dissecting mosquito innate immune responses to arbovirus infection. The Journal of
845 general virology. 2009;90(Pt 9):2061-72. doi: 10.1099/vir.0.013201-0.
846 66. Zhang X, Aksoy E, Girke T, Raikhel AS, Karginov FV. Transcriptome-wide
847 microRNA and target dynamics in the fat body during the gonadotrophic cycle of Aedes
848 aegypti. Proceedings of the National Academy of Sciences of the United States of
849 America. 2017;114(10):E1895-E903. doi: 10.1073/pnas.1701474114.
850 67. Barletta AB, Nascimento-Silva MC, Talyuli OA, Oliveira JH, Pereira LO, Oliveira
851 PL, et al. Microbiota activates IMD pathway and limits Sindbis infection in Aedes
852 aegypti. Parasit Vectors. 2017;10(1):103. Epub 2017/02/25. doi: 10.1186/s13071-017-
853 2040-9.
854 68. Kumar A, Srivastava P, Sirisena P, Dubey SK, Kumar R, Shrinet J, et al.
855 Mosquito Innate Immunity. Insects. 2018;9(3). Epub 2018/08/12. doi:
856 10.3390/insects9030095.
857 69. Friedrich N, Hagedorn M, Soldati-Favre D, Soldati T. Prison break: pathogens
858 strategies to egress from host cells. Microbiol Mol Biol Rev. 2012;76(4):707-20. doi:
859 10.1128/MMBR.00024-12.
860 70. Narasimhan S, Rajeevan N, Liu L, Zhao YO, Heisig J, Pan J, et al. Gut
861 Microbiota of the Tick Vector Ixodes scapularis Modulate Colonization of the Lyme

862 Disease Spirochete. Cell Host & Microbe. 2014;15(1):58-71. doi:
863 10.1016/j.chom.2013.12.001.
864 71. Rodgers FH, Gendrin M, Wyer CAS, Christophides GK. Microbiota-induced
865 peritrophic matrix regulates midgut homeostasis and prevents systemic infection of
866 malaria vector mosquitoes. PLOS Pathogens. 2017;13(5):e1006391. doi:
867 10.1371/journal.ppat.1006391.
868 72. Gusmão DS, Santos AV, Marini DC, Bacci Jr M, Berbert-Molina MA, Lemos FJA.
869 Culture-dependent and culture-independent characterization of microorganisms
870 associated with Aedes aegypti (Diptera: Culicidae) (L.) and dynamics of bacterial
871 colonization in the midgut. Acta Tropica. 2010;115(3):275-81. doi:
872 10.1016/j.actatropica.2010.04.011.
873 73. Tsai YL, Hayward RE, Langer RC, Fidock DA, Vinetz JM. Disruption of
874 Plasmodium falciparum Chitinase Markedly Impairs Parasite Invasion of Mosquito
875 Midgut. Infection and Immunity. 2001;69(6):4048-54. doi: 10.1128/IAI.69.6.4048-
876 4054.2001.
877 74. Goebel W, Gross R. Intracellular survival strategies of mutualistic and parasitic
878 prokaryotes. Trends Microbiol. 2001;9(6):267-73. Epub 2001/06/08.
879 75. Kumar S, Molina-Cruz A, Gupta L, Rodrigues J, Barillas-Mury C. A
880 peroxidase/dual oxidase system modulates midgut epithelial immunity in *Anopheles*
881 *gambiae*. Science. 2010;327(5973):1644-8. doi: 10.1126/science.1184008.
882 76. Brady C, Cleenwerck I, Venter S, Coutinho T, De Vos P. Taxonomic evaluation
883 of the genus Enterobacter based on multilocus sequence analysis (MLSA): Proposal to
884 reclassify E. nimipressuralis and E. amnigenus into Lelliottia gen. nov. as Lelliottia

885 nimipressuralis comb. nov. and Lelliottia amnigena comb. nov., respectively, E.
886 gergoviae and E. pyrinus into Pluralibacter gen. nov. as Pluralibacter gergoviae comb.
887 nov. and Pluralibacter pyrinus comb. nov., respectively, E. cowanii, E. radicincitans, E.
888 oryzae and E. arachidis into Kosakonia gen. nov. as Kosakonia cowanii comb. nov.,
889 Kosakonia radicincitans comb. nov., Kosakonia oryzae comb. nov. and Kosakonia
890 arachidis comb. nov., respectively, and E. turicensis, E. helveticus and E. pulveris into
891 Cronobacter as Cronobacter zurichensis nom. nov., Cronobacter helveticus comb. nov.
892 and Cronobacter pulveris comb. nov., respectively, and emended description of the
893 genera Enterobacter and Cronobacter. Systematic and Applied Microbiology.
894 2013;36(5):309-19. doi: https://doi.org/10.1016/j.syapm.2013.03.005.
895 77. Gouy M, Guindon S, Gascuel O. SeaView version 4: A multiplatform graphical
896 user interface for sequence alignment and phylogenetic tree building. Molecular biology
897 and evolution. 2010;27(2):221-4. Epub 2009/10/23. doi: 10.1093/molbev/msp259.
898 78. Peleg J. Growth of arboviruses in primary tissue culture of Aedes aegypti
899 embryos. Am J Trop Med Hyg. 1968;17.
900 79. Horn T, Boutros M. E-RNAi: a web application for the multi-species design of
901 RNAi reagents--2010 update. Nucleic Acids Research. 2010;38(Web Server
902 issue):W332-9. doi: 10.1093/nar/gkq317.
903 80. Livak KJ, Schmittgen TD. Analysis of Relative Gene Expression Data Using
904 Real-Time Quantitative PCR and the 2−ΔΔCT Method. Methods (San Diego, Calif).
905 2001;25(4):402-8. doi: 10.1006/meth.2001.1262.
906 81. Isoe J, Collins J, Badgandi H, Day WA, Miesfeld RL. Defects in coatomer protein
907 I (COPI) transport cause blood feeding-induced mortality in Yellow Fever mosquitoes.

908 Proceedings of the National Academy of Sciences of the United States of America.
909 2011;108(24):E211-7. doi: 10.1073/pnas.1102637108.
910 82. Saldaña MA, Etebari K, Hart CE, Widen SG, Wood TG, Thangamani S, et al.
911 Zika virus alters the microRNA expression profile and elicits an RNAi response in Aedes
912 aegypti mosquitoes. PLoS Neglected Tropical Diseases. 2017;11(7):e0005760-18. doi:
913 10.1371/journal.pntd.0005760.
914 83. Coon KL, Vogel KJ, Brown MR, Strand MR. Mosquitoes rely on their gut
915 microbiota for development. Molecular Ecology. 2014;23(11):2727-39. doi:
916 10.1111/mec.12771.
917
918

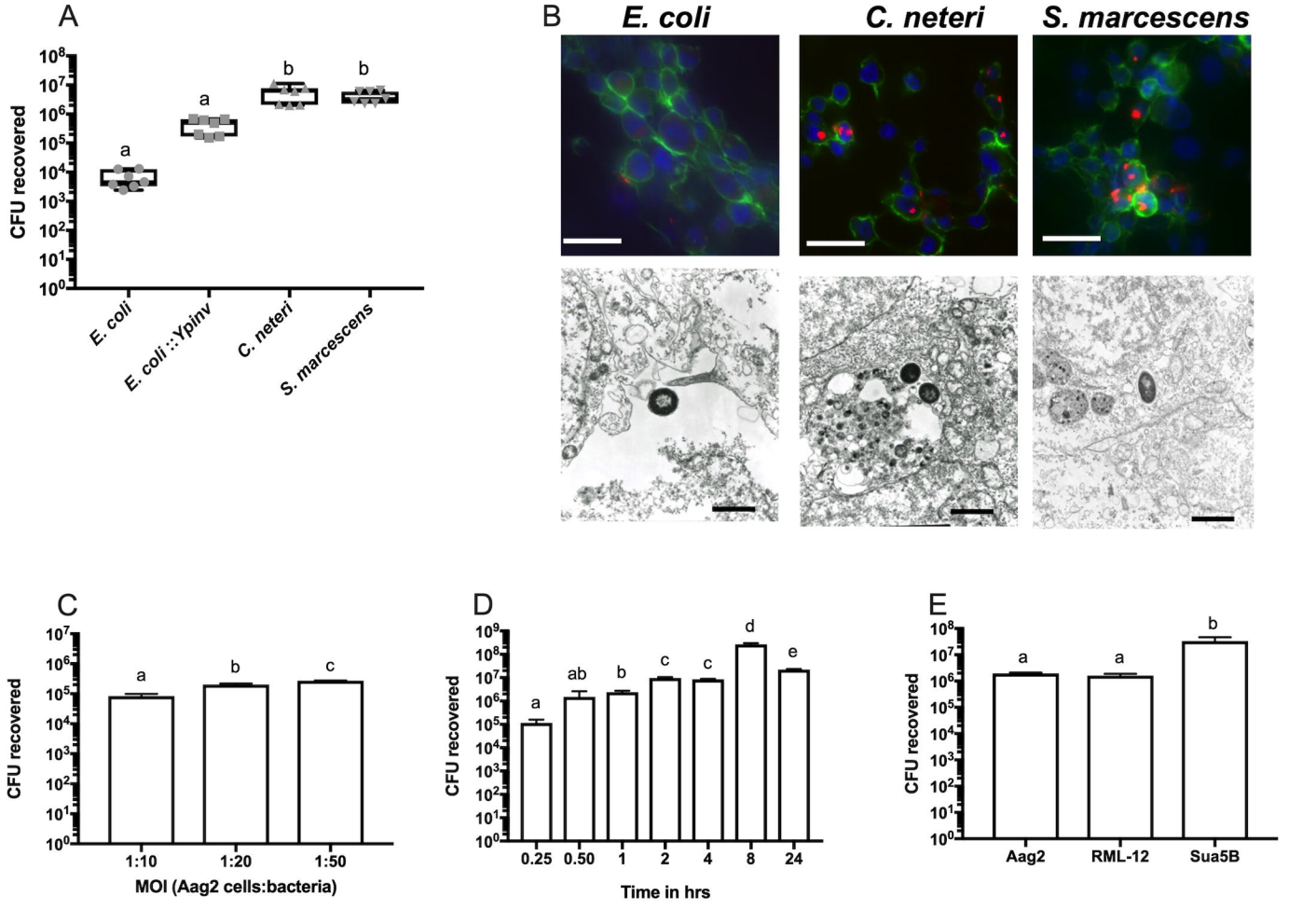
A
CFU recovered
10^8
10^7
10^6
10^5
10^4
10^3
10^2
10^1
10^0
a
a
b
b
E. coli
E. coli ::Ypinv
C. neteri
S. marcescens
B
E. coli
C. neteri
S. marcescens
C
CFU recovered
10^7
10^6
10^5
10^4
10^3
10^2
10^1
10^0
a
b
c
1:10
1:20
1:50
MOI (Aag2 cells:bacteria)
D
CFU recovered
10^9
10^8
10^7
10^6
10^5
10^4
10^3
10^2
10^1
10^0
a
ab
b
c
c
d
e
0.25
0.50
1
2
4
8
24
Time in hrs
E
CFU recovered
10^8
10^7
10^6
10^5
10^4
10^3
10^2
10^1
10^0
a
a
b
Aag2
RML-12
Sua5B

A

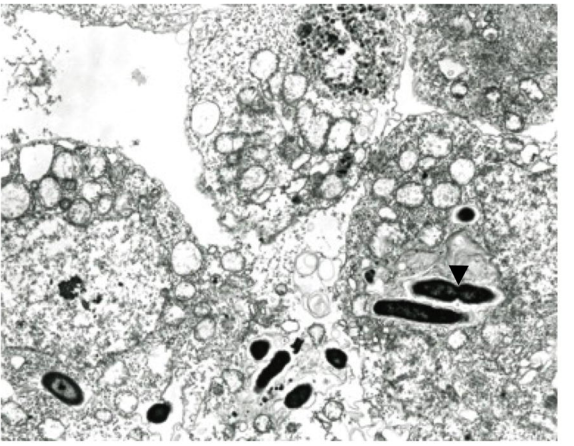

B

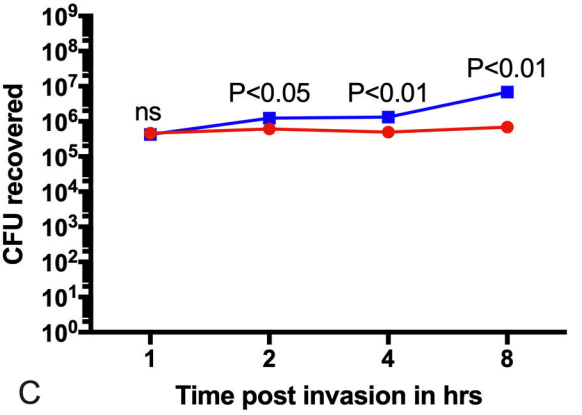
CFU recovered
10^9
10^8
10^7
10^6
10^5
10^4
10^3
10^2
10^1
10^0
ns
P<0.05
P<0.01
P<0.01
1
2
4
8
Time post invasion in hrs

C

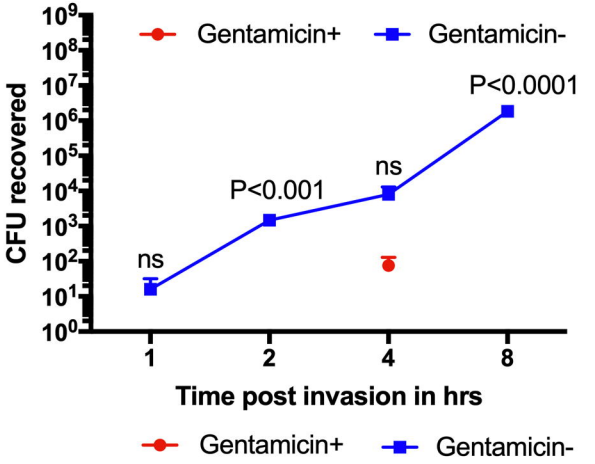
Gentamicin+
Gentamicin-
CFU recovered
10^9
10^8
10^7
10^6
10^5
10^4
10^3
10^2
10^1
10^0
ns
P<0.001
ns
P<0.0001
1
2
4
8
Time post invasion in hrs
Gentamicin+
Gentamicin-

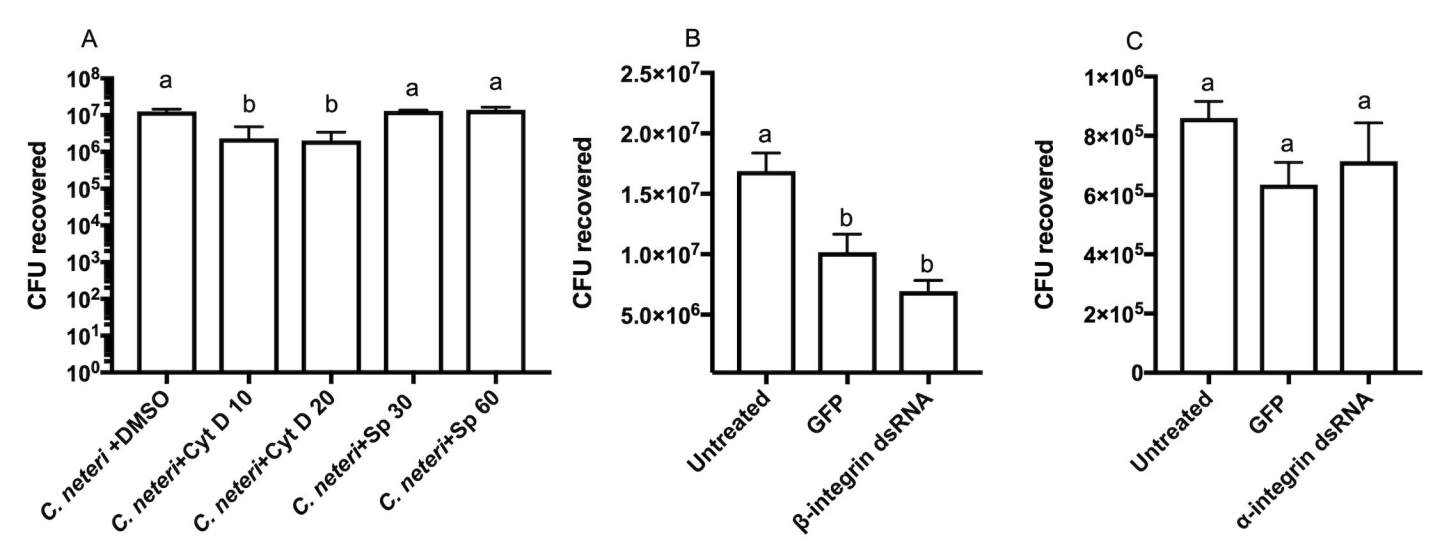
A
CFU recovered
10^8
10^7
10^6
10^5
10^4
10^3
10^2
10^1
10^0
a
b
b
a
a
C. neteri +DMSO
C. neteri+Cyt D 10
C. neteri+Cyt D 20
C. neteri+Sp 30
C. neteri+Sp 60
B
CFU recovered
2.5×10^7
2.0×10^7
1.5×10^7
1.0×10^7
5.0×10^6
a
b
b
Untreated
GFP
β-integrin dsRNA
C
CFU recovered
1×10^6
8×10^5
6×10^5
4×10^5
2×10^5
0
a
a
a
Untreated
GFP
α-integrin dsRNA

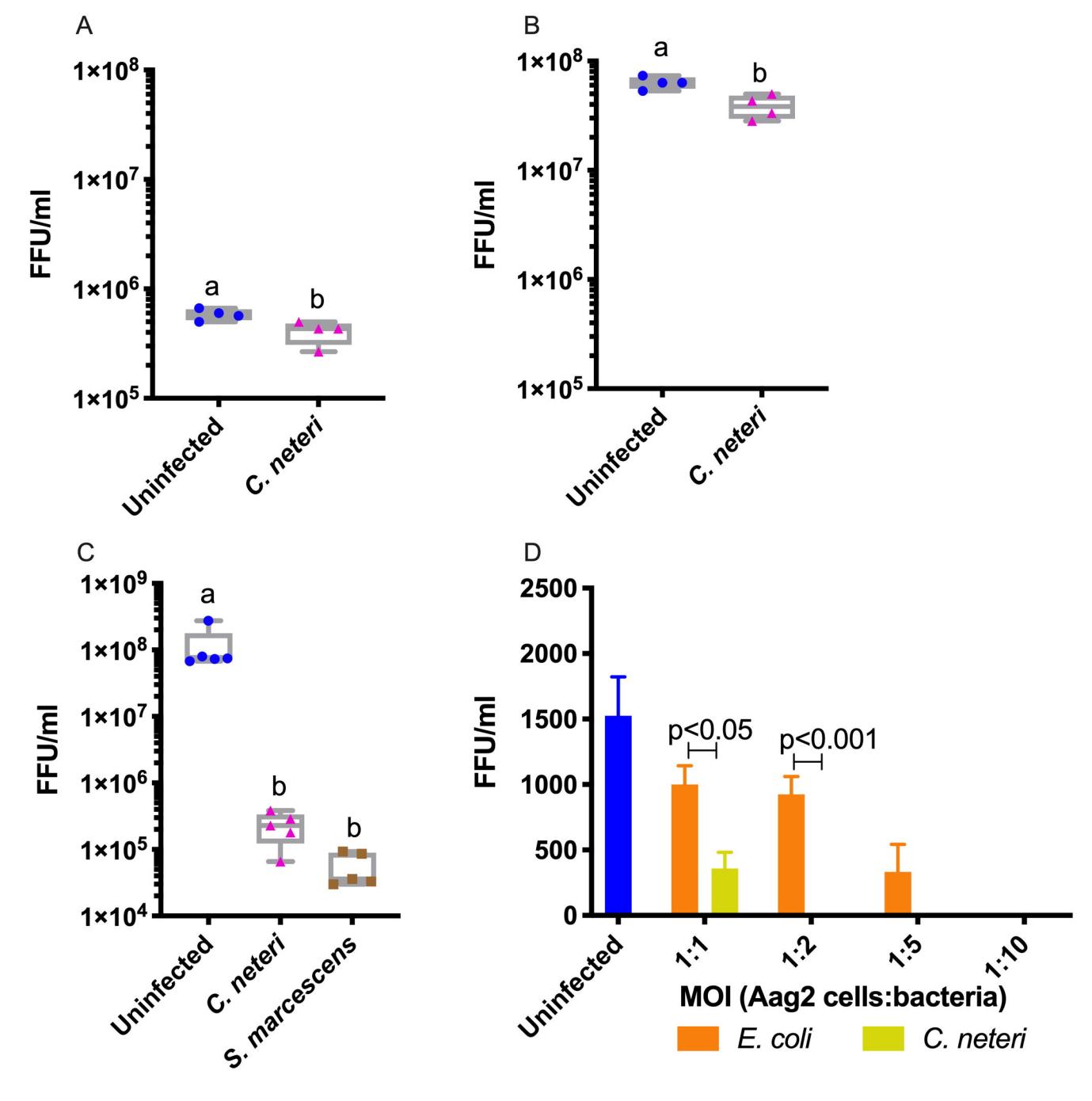
A
1×10^8
1×10^7
1×10^6
1×10^5
FFU/ml
a
b
Uninfected
C. neteri
B
1×10^8
1×10^7
1×10^6
1×10^5
FFU/ml
a
b
Uninfected
C. neteri
C
1×10^9
1×10^8
1×10^7
1×10^6
1×10^5
1×10^4
FFU/ml
a
b
b
Uninfected
C. neteri
S. marcescens
D
2500
2000
1500
1000
500
0
FFU/ml
p<0.05
p<0.001
Uninfected
1:1
1:2
1:5
1:10
MOI (Aag2 cells:bacteria)
E. coli
C. neteri

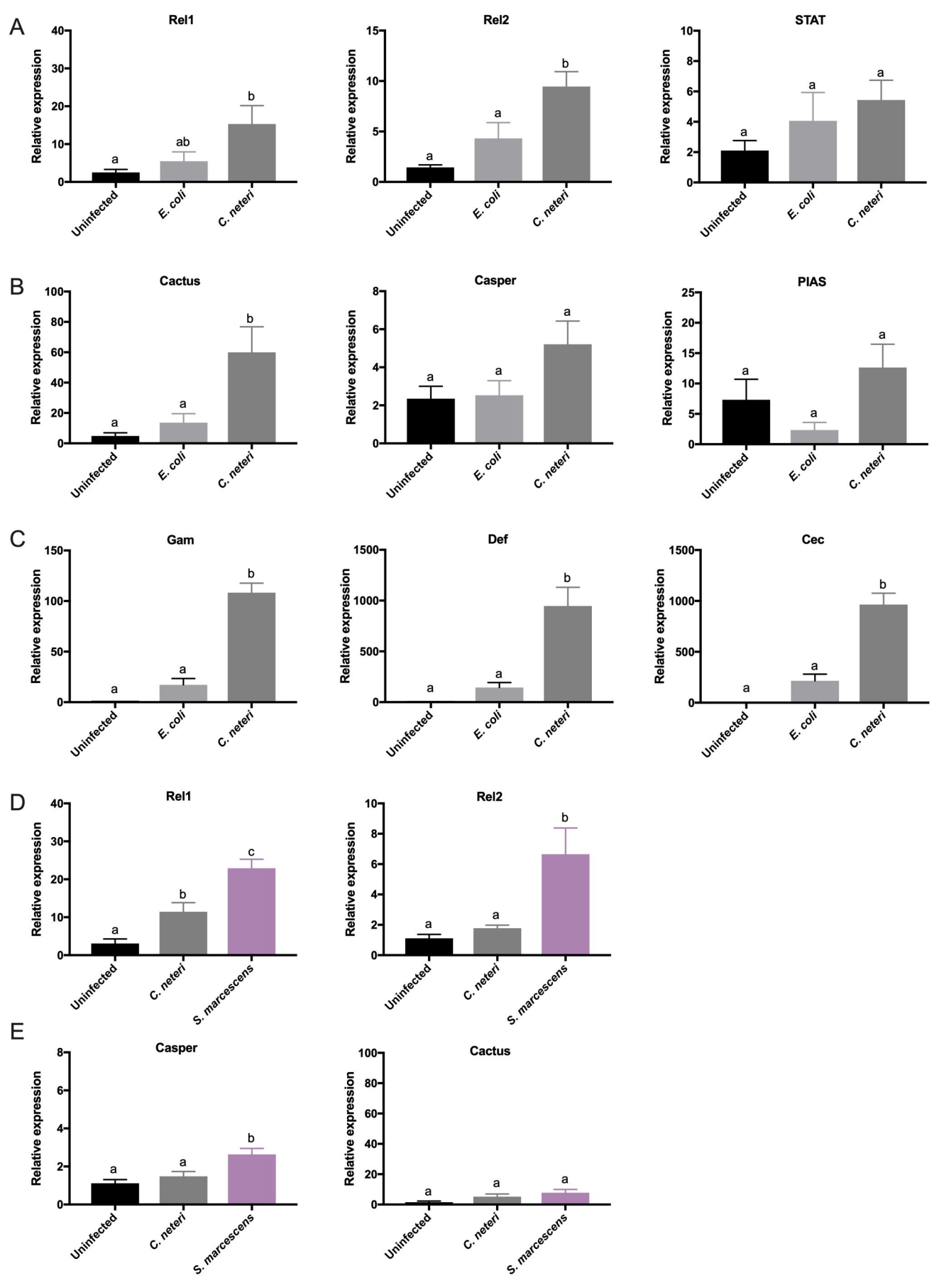
A
Rel1
Relative expression
40
30
20
10
0
a
ab
b
Uninfected
E. coli
C. neteri
Rel2
Relative expression
15
10
5
0
a
a
b
Uninfected
E. coli
C. neteri
STAT
Relative expression
10
8
6
4
2
0
a
a
a
Uninfected
E. coli
C. neteri
B
Cactus
Relative expression
100
80
60
40
20
0
a
a
b
Uninfected
E. coli
C. neteri
Casper
Relative expression
8
6
4
2
0
a
a
a
Uninfected
E. coli
C. neteri
PIAS
Relative expression
25
20
15
10
5
0
a
a
a
Uninfected
E. coli
C. neteri
C
Gam
Relative expression
150
100
50
0
a
a
b
Uninfected
E. coli
C. neteri
Def
Relative expression
1500
1000
500
0
a
a
b
Uninfected
E. coli
C. neteri
Cec
Relative expression
1500
1000
500
0
a
a
b
Uninfected
E. coli
C. neteri
D
Rel1
Relative expression
40
30
20
10
0
a
b
c
Uninfected
C. neteri
S. marcescens
Rel2
Relative expression
10
8
6
4
2
0
a
a
b
Uninfected
C. neteri
S. marcescens
E
Casper
Relative expression
8
6
4
2
0
a
a
b
Uninfected
C. neteri
S. marcescens
Cactus
Relative expression
100
80
60
40
20
0
a
a
a
Uninfected
C. neteri
S. marcescens

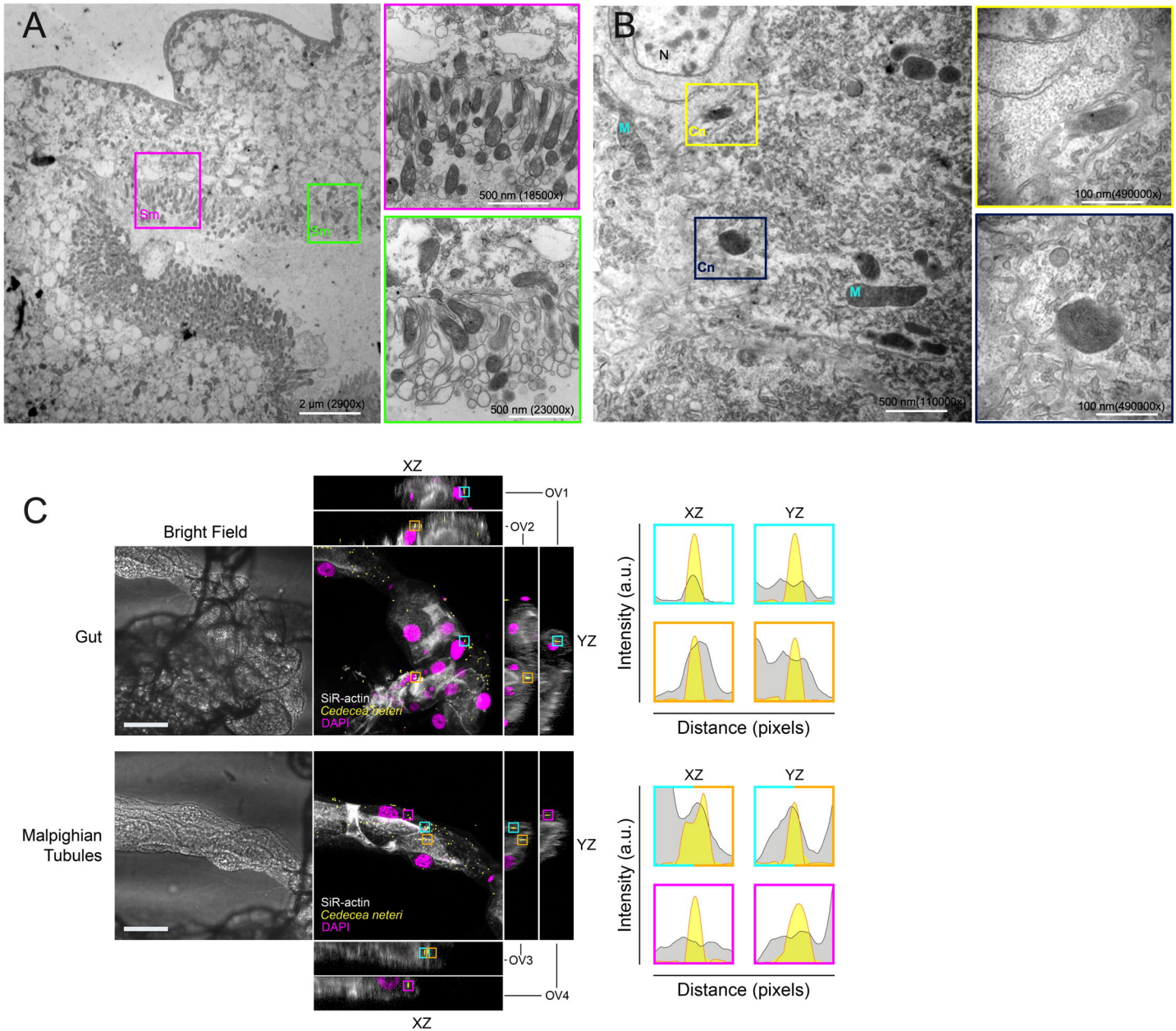
A
Sm
Cn
500 nm (18500x)
500 nm (23000x)
2 µm (2900x)
B
N
M
Cn
Cn
M
100 nm(490000x)
100 nm(490000x)
500 nm(110000x)
C
XZ
OV1
OV2
Bright Field
Gut
YZ
SiR-actin
Cedecea neteri
DAPI
Malpighian Tubules
YZ
SiR-actin
Cedecea neteri
DAPI
OV3
OV4
XZ
XZ
YZ
Intensity (a.u.)
Distance (pixels)
XZ
YZ
Intensity (a.u.)
Distance (pixels)